

THE FLORIDA STATE UNIVERSITY
COLLEGE OF ARTS AND SCIENCES

ESTIMATES OF OCEANIC HEAT
TRANSPORT IN THE TROPICAL PACIFIC:
Mean, Seasonal and Interannual Variability

by

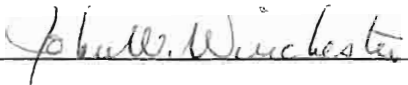
ALEJANDRO F. PARES-SIERRA

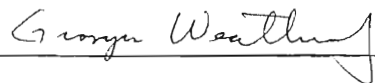
A thesis submitted to the
Department of Oceanography
in partial fulfillment of the
requirements for the degree of
Master of Science

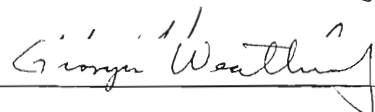
Approved:

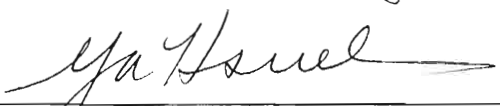


Professor Directing Thesis









Chairman, Department of Oceanography

August 1984

August, 1984

Abstract

Meridional heat transport in the tropical Pacific is estimated using a linear numerical transport model with realistic boundaries and forced by 18 years of observed wind covering the period from January 1962 to December 1979. The long-term mean heat transport estimated in this study is similar to the estimates based on heat balance and radiation considerations and on complex numerical models which account for thermodynamics as well. This points to the dominant role played by the adiabatic process, the only heat transport mechanism present in this study, in the heat balance for the equatorial Pacific.

The combined Ekman and geostrophic heat transport can account for the net meridional heat transport except near the equator where continuity requirements dictate. The Ekman and geostrophic transports oppose each other, and their small difference in magnitude gives rise to the net meridional heat transport, resulting in transport away from the equator for the southern hemisphere and north of 6°N while for the band between 6°N and the equator an equatorward transport is present.

Seasonal and interannual variations are found to be as large or even larger than the long-term mean. Seasonal variations in meridional heat transport are in accordance with seasonal variations in zonal winds via Ekman transport, while the geostrophic transport meridional heat transport are in accordance with seasonal variations in zonal winds via Ekman transport, while the geostrophic transport remains more or less constant on this time scale. The results are

a net poleward heat transport in the winter hemisphere and a net equatorward transport in the summer hemisphere.

At the interannual time scale, variabilities in both Ekman and geostrophic components contribute to the interannual variability in heat transport. Major features of the interannual variations in meridional heat transport appear to be associated with the El Nino events. It is interesting to note that the interannual variations associated with El Nino events are not restricted to the near-equatorial region. Phase locking between the interannual variations and the annual cycle is evident in the data set.

Major findings in this study based on an adiabatic model are expected to carry over to more realistic non-linear numerical models.

Acknowledgments

This work was supported by the National Science Foundation Grant OCE 8119052.

I wish to express my most sincere gratitude to Dr. J. O'Brien. His guidance and encouragement throughout the past two years made this research possible. I am also grateful of the time taken by Drs. John Winchester, Georges Weatherly and Wilton Sturges while serving on my thesis committee. The method to estimate heat flux use in this study was suggested by Dr. Kirk Bryan.

In addition, sincere appreciation is extended to my colleagues of the Air-Sea Interaction Group for their criticisms and suggestions. Very especially I want to acknowledge the invaluable help of Dr. Masamichi Inoue during the whole process of doing this thesis.

I wish to thank Helen McKelder for typing both the early draft versions and the final manuscript.

Finally, I would like to thank my parents and my wife, Irma. Their love, support and understanding have formed the good part of me. I dedicate this thesis to them.

Table of Contents

	Page
ABSTRACT	ii
ACKNOWLEDGMENTS	iv
TABLE OF CONTENTS	v
LIST OF FIGURES	vi
I. INTRODUCTION	1
II. PROCEDURES	
a. NET HEAT TRANSPORT	7
b. COMPONENTS OF OCEANIC HEAT TRANSPORT	11
III. RESULTS AND DISCUSSION	
a. NET MERIDIONAL TRANSPORT	15
b. SEASONAL VARIATION	25
c. INTERANNUAL VARIATION	35
IV. SUMMARY AND CONCLUSIONS	42
REFERENCES	46
APPENDIX	49

List of Figures

		Page
Fig. 1	Comparison of model geometry with the tropical Pacific Ocean. The model basin extends from 18°N to 12°S and 126°E to 79°W (Fig. 1 of Busalacchi and O'Brien, 1980).	8
Fig. 2	Mean net meridional heat transport by the ocean model. Northward transport positive. Units are in PW (1 PW = 10^{15} W).	17
Fig. 3	January-July average heat transport by the ocean model compared to the January-July estimates from Bryan (1982a). Units are in PW.	19
Fig. 4	Mean meridional heat transport due to: (a) Ekman effect; (b) geostrophic effect; (c) Ekman + geostrophic; (d) net transport. See text for definitions. Note different units for a-b and c-d.	22
Fig. 5	Zonally averaged mean east-west pseudo wind stress [wind magnitude times wind component (Goldenberg and O'Brien, 1981)]. Negative values indicate westward winds. Units are (Goldenberg and O'Brien, 1981)]. Negative values indicate westward winds. Units are in $10^2 \text{ m}^2\text{s}^{-2}$.	23

	Page	
Fig. 6a	Monthly mean zonally averaged east-west wind pseudo stress. Positive values indicates eastward winds. Units are in m^2s^{-2} . Contour interval is $3 m^2s^{-2}$.	28
Fig. 6b	Monthly mean zonally averaged east-west wind pseudo stress anomaly. Zonal mean at each latitude has been removed. Negative contours (dash lines) indicate stronger than average easterlies. Contour interval is $3 m^2s^{-2}$.	29
Fig. 7	Annual cycle of net meridional heat transport. Positive contours indicate northward transport. Units are in PW. Contour interval is .1 PW.	31
Fig. 8	Annual cycle of meridional heat transport due to Ekman transport. Positive contours indicate northward transport. Units are in PW time $10 (10^{16}W)$. Contour interval is .4 PW.	32
Fig. 9	Annual cycle of meridional heat transport due to geostrophic transport. Positive contours indicate northward transport. Units are in 10^{16} Watts. Contour interval is .4 PW.	33
	indicate northward transport. Units are in 10^{16} Watts. Contour interval is .4 PW.	33

- Fig. 10a Interannual variability of the net meridional heat transport obtained by filtering with a 12-month running mean. The years that have been classified as El Nino years are shaded in the figure. Units are in PW. Contour interval is .1 PW. 38
- Fig. 10b Same as Fig. 10a, but for the heat transport anomaly. 39

I. Introduction

The earth receives shortwave radiation from the sun predominantly in the tropics, but longwave radiation back into space is relatively uniform over the globe. This results in a heat gain at low latitudes and a heat loss at high latitudes. Due to this differential heating, a net poleward heat transport by the earth's fluid envelope is required. Over continents, redistribution of energy takes place exclusively in the atmosphere while over the oceans, both, the ocean and the atmosphere intervene. The relative importance of the atmosphere and ocean in effecting this transport has not yet been established. Recent results suggest, however, that the ocean heat transport is not only a relevant mechanism, but, in some areas, provides the dominant transport (Vonder Haar and Oort, 1973). Using radiation budget calculations Oort and Vonder Haar (1976) found that the oceanic contribution to the total net poleward heat transport at 20°N is about 50%. This percentage seems to increase equatorward, while at middle and high latitudes the atmospheric contribution seems dominant.

Heat exchange through the ocean-atmosphere interface is a primary driving force for the atmospheric circulation; wind stresses at the ocean surface, in turn, drive the major ocean currents. An important component of this feedback mechanism must be the

redistribution of heat by the ocean. A better understanding of the oceanic heat transport (OHT) mechanisms seems necessary in order to effectively model and predict climate.

Oort and Vonder Haar (1976) showed evidence of a large annual cycle of OHT at low latitudes with heat flowing from the summer to the winter hemisphere. They found that a cross equatorial seasonally varying heat flux of the order of 8 PW ($1 \text{ PW} = 10^{15} \text{ W}$) is needed to maintain the heat balance. This large necessary heat flux shows the primary role played by the tropical ocean in the earth's climate. Since the pioneering work of Oort and Vonder Haar (1976), widespread attention has been given to the subject. Recent reviews of the progress in calculating OHT were presented by Bryan (1982b, 1983).

Three basic methods have been used to estimate OHT (Bryan, 1983). The first one is the heat balance method. Implementation of this method has followed two different approaches: heat balance considerations at the ocean surface and a global heat balance. In the former, empirical formulas are used to compute heat fluxes through the ocean surface while in the latter a global heat balance of the entire ocean-atmosphere-earth system is considered. In both cases, transport of heat by the ocean is estimated as a residual term from the requirement of heat balance. The advantage of this method is that it permits an estimation of the heat balance method is that it permits an estimation of the heat balance

components for large areas of the ocean using standard meteorological-oceanographic observations. A disadvantage of this method is that the uncertainties in the parameterization of surface heat fluxes create unknown uncertainties in the estimated transport. This is the "traditional method" (Hall and Bryden, 1982), and it has been used by a number of investigators (e.g., Budyko, 1963; Wyrcki, 1965; Oort and Vonder Haar, 1976; Hasteranth and Lamb, 1977).

A second method is the direct method. It uses oceanographic observations of velocity and temperature to calculate direct heat fluxes. This method permits investigation into the mechanisms by which heat is transported (Bryan, 1983). Although the direct method seems to be most appropriate, the lack of detailed hydrographic or direct current measurements across an entire ocean makes its use very limited. Nevertheless, its value lies in the fact that it gives "direct observations" of heat transport against which other indirect calculations or models can be compared. Reviews on the direct estimates and mechanisms of OHT was presented by Hall and Bryden (1982).

A third possible way of estimating OHT is through the use of numerical models. The problem of constructing a simple model for OHT is basically the same as finding a simple model of the ocean circulation (Bryan, 1982b). As with most models, models of heat transport can be classified into two overlapping categories: heat transport can be classified into two overlapping categories:

those that try to isolate basic physical mechanisms (e.g., Schopf, 1980; Cane and Sarachik, 1983) and those that try to reproduce observed data (e.g., Bryan et al., 1975; Bryan and Lewis, 1979). In this study, an intermediate approach is taken: A simple, linear, reduced-gravity model but with realistic geometry and forced by real winds, is used to estimate heat transports. The objective of this study is to understand better how the tropical Pacific Ocean transports heat away from the equator.

Cane and Sarachik (1981) solved the linear shallow water equation forced by latitudinally varying (but zonally averaged) seasonal wind. Estimating heat transports with this model they found (Cane and Sarachik, 1983) that the meridional transport by the western boundary current is of the same magnitude as but out of phase with the seasonally varying interior transport, and both tend to cancel each other. The role of Ekman flow and planetary waves on the OHT has been investigated by Schopf (1980). Using a numerical model, Schopf found that basic Ekman pumping and drift could account for most of the net cross-equatorial heat flux. He also found that additions of planetary and gravity waves do not alter the basic pattern. The values of OHT were found to be comparable to those estimated by Oort and Vonder Haar (1976) (Schopf, 1980). Schopf points out that the adiabatic advection mechanism for heat transport implicit in his model would not be appropriate for higher latitudes implicit in his model would not be appropriate for higher latitudes

(>20°) where other physics should be included (i.e., surface heat fluxes, mixing processes, gyral effect, etc.).

The present study is somewhat similar to that of Schopf (1980) and Cane and Sarachik (1983): estimation of oceanic heat fluxes are drawn from a simple numerical model. Our study differs from theirs, however, in that our model includes the realistic boundaries of the equatorial Pacific and is forced by real winds.

The same model has been used before to study the seasonal (Busalacchi and O'Brien, 1980) and interannual variability of the equatorial Pacific for the 60's (Busalacchi and O'Brien, 1981) and 70's (Busalacchi et al., 1983).

A very good agreement with observations of the thermocline topography and its seasonal variations was obtained when the model was forced by mean monthly winds (Busalacchi and O'Brien, 1980). Using 18 years of observed winds covering the period 1961-1978, the variability of sea level at the Galapagos Island was found to be similar to the variability of the model pycnocline. El Nino events of the 60's and 70's are characterized in the model by a persistently deep pycnocline. The results also indicate that the variability at the equator is related to the excitation and propagation of Kelvin and Rossby waves (Busalacchi and O'Brien, 1981).

For the present study the same wind data, extended to 1979 is used to force the model. A description of the procedures used to estimate OHT is presented in section 2. In section 3 the results are presented and discussed. Comparison with other authors' results is also given in this section. Finally, in section 4, conclusions and criticisms are considered.

II. Procedures

a. Net heat transport

In this study the model developed by Busalacchi and O'Brien, (1980, 1981) was used to compute heat transport. The model is a one-layer, reduced-gravity linear transport model on an equatorial β -plane. The model covers a domain extending from 126°E to 79°W and from 18°N to 12°S with idealized boundaries to represent the tropical Pacific Ocean (Fig. 1). The northern and southern boundaries are treated as open boundaries.

Through the equation of state, the difference in density between the two layers is related to a difference in temperature and heat content. For the upper layer of thickness h and temperature T , the heat content per unit area, s , can be expressed as

$$s = \rho c_p (T - T_0) h, \quad (1)$$

where ρ is the density of the upper layer, c_p is the heat capacity and T_0 is the reference temperature (temperature of the lower layer).

Using the equation of state in the form

$$\rho = \rho_0 (1 - \alpha(T - T_0)) \quad (2)$$

where ρ_0 is the reference density and α is the coefficient of thermal expansion. $(T - T_0)$ can be eliminated from (1) to give an expression for where ρ_0 is the reference density and α is the coefficient of thermal expansion, $(T - T_0)$ can be eliminated from (1) to give an expression for heat content in terms of the density jump $\Delta\rho = \rho_0 - \rho$ and the layer

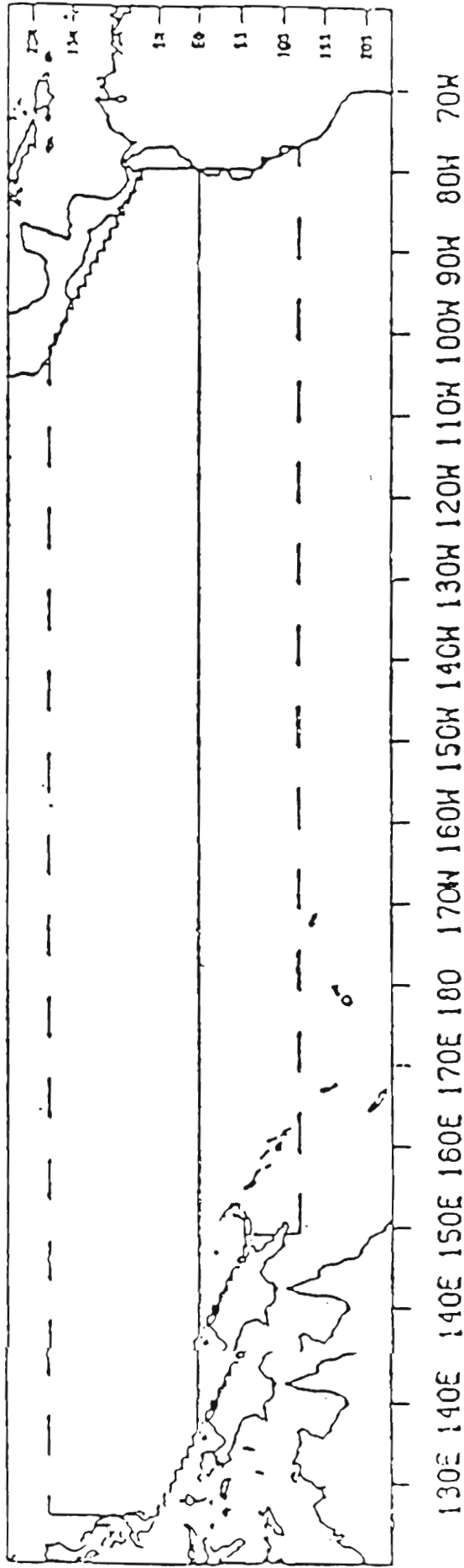


Fig. 1 Comparison of model geometry with the tropical Pacific Ocean. The model basin extends from 18°N to 12°S and 126°E to 79°W (Fig. 1 of Busalacchi and O'Brien, 1980).

thickness

$$s = \frac{\rho}{\rho_0} c_p \frac{\Delta\rho}{\alpha} h. \quad (3)$$

If one approximates ρ/ρ_0 to 1, one can write the rate of change of the estimated heat content, s ,

$$\frac{\partial s}{\partial t} = \gamma \frac{\partial h}{\partial t} \quad (4)$$

where $\gamma = c_p \frac{\Delta\rho}{\alpha}$ is taken to be a constant in this study. A list of symbols may be found in the Appendix. Eq. (4) implies that the thickness of the layer can be considered as a proxy for heat content. If we integrate this last equation across a latitudinal band extending from the western boundary to the eastern boundary of a basin and north-south between latitudes, $y_0 \pm \Delta y$, we obtain an expression for the rate of total storage of heat in the latitudinal strip as

$$\frac{\partial S}{\partial t} = \gamma \int_x \int_y \frac{\partial h}{\partial t} dy dx, \quad (5)$$

where

$$S = \int_x \int_y s dy dx, \quad (6)$$

is the amount of heat in the volume and the integration is taken from x_0 to x_{00} (meridional boundaries of the basin) and from $y_0 - \Delta y$ to $y_0 + \Delta y$ (southern and northern edges of the band).

$y_0 + \Delta y$ (southern and northern edges of the band).

Following Busalacchi and O' Brien (1980), the ocean model equations are

$$\frac{\partial V}{\partial t} = -\beta y U - c^2 \frac{\partial h}{\partial y} + \frac{\tau^y}{\rho} + A \nabla^2 V, \quad (7a)$$

$$\frac{\partial U}{\partial t} = \beta y V - c^2 \frac{\partial h}{\partial x} + \frac{\tau^x}{\rho} + A \nabla^2 U, \quad (7b)$$

$$\frac{\partial h}{\partial t} + \frac{\partial U}{\partial x} + \frac{\partial V}{\partial y} = 0, \quad (7c)$$

where $V=Hv$ and $U=Hu$ are the transports in the north-south and east-west directions, respectively, H is the undisturbed depth of the layer, c is the baroclinic phase speed taken to be 2.45ms^{-1} , τ is the wind stress applied as a body force, and A is the horizontal eddy viscosity coefficient to make the horizontal velocity along the closed boundaries vanish.

If we integrate the continuity equation (7c) over the equatorial strip, we obtain, after multiplication by γ , and using (5).

$$\frac{\partial S}{\partial t} = -\gamma \int_x \int_y \left[\frac{\partial U}{\partial x} + \frac{\partial V}{\partial y} \right] dy dx,$$

$$\frac{\partial S}{\partial t} = -\gamma \left[\int_y [U]_{x_0}^{x_0+\Delta x} dy \right] - \gamma \left[\int_x [V]_{y_0-\Delta y}^{y_0+\Delta y} dx \right].$$

$$\frac{\partial S}{\partial t} = -\gamma \left[\int_y [U]_{x_0}^{x_0+\Delta x} dy \right] - \gamma \left[\int_x [V]_{y_0-\Delta y}^{y_0+\Delta y} dx \right].$$

Since at the eastern and western boundaries the normal transport is zero, we get for the rate of heat storage

$$\frac{\partial S}{\partial t} = B(y_0 - \Delta y) - B(y_0 + \Delta y), \quad (8a)$$

where

$$B(y) = \gamma \int_{x_0}^{x_{00}} V(x, y) dx \quad (8b)$$

The first and second terms on the righthand side of (8a) can be identified as the northward heat transports at the southern and northern boundaries of the band, respectively.

b. Components of oceanic heat transport

For a basin closed at one end, two important modes of meridional heat transport can be identified (Bryan, 1982b):

- i) Overturning in the meridional plane, where poleward heat transport can take place due to the poleward movement of warm water at the surface compensated by the equatorial movement of colder deep water.
- ii) Gyre effect, where correlations between velocities and temperature in the horizontal plane contribute to a meridional heat transport.

At low latitudes the temperature contrast between surface and deep water is much greater than the temperature contrast in a typical east-west section. Meridional overturning is therefore more efficient in transporting heat than a gyre circulation of similar east-west section. Meridional overturning is therefore more efficient in transporting heat than a gyre circulation of similar

strength. Earlier calculations (e.g. Bryan and Lewis, 1979; Meehl et al., 1982) seem to corroborate this idea.

Meridional overturning is the only mechanism included in a one-layer, reduced-gravity model. In this model, net meridional transport in the upper layer is compensated by an equal transport in the opposite direction, of higher density (colder) water in the lower layer. Away from the equator, the overturning circulation can be thought of as being composed of two components. One is related to the Ekman transport and the other is a geostrophically balanced component.

For low-frequency forcing, away from the equator and boundaries, the system of equations (7a) and (7b) can be approximated as (Busalacchi and O'Brien, 1980):

$$\beta y U = -c^2 \frac{\partial h}{\partial y} + \frac{\tau y}{\rho}, \quad (9)$$

$$-\beta y V = -c^2 \frac{\partial h}{\partial x} + \frac{\tau x}{\rho}. \quad (10)$$

For this linear model one can think of the transports U and V as being composed of two components satisfying the geostrophic and Ekman relations. Meridional heat transport contributions due to Ekman (B_E) and geostrophic (B_g) components are defined as:

$$B_E(y,t) = \gamma \int_{x_0}^{x_0} V_E dx, \quad (11)$$

$$B_g(y, t) = \gamma \int_{x_0}^{x_{00}} V_g dx, \quad (12)$$

where V_E and V_g refer to the transport due to Ekman and geostrophic components, respectively, and are defined as:

$$V_E = - \frac{\tau_x}{\beta y \rho} ; V_g = \frac{c^2}{\beta y} \frac{\partial h}{\partial x} . \quad (13)$$

Away from the equator these two contributions must nearly sum up to the net transport. The integrated geostrophic transport depends on large scale features that adjust in much longer time than the adjustment time for the Ekman transport. It can be expected that most of the seasonal and shorter time scales variability in the net meridional transport is related to the Ekman transport changes. On the other hand, for the interannual variability, the geostrophic component is more likely to be important.

At the equator the vanishing of the Coriolis force enables one to write an equation for V in the form (Busalacchi and O'Brien, 1980)

$$V_{yyt} - \frac{\beta^2 y^2}{c^2} V_t + \beta V_x = k \cdot \left(\nabla_x \frac{\tau}{\rho} \right)_x + \frac{\beta y}{c^2} \left(\frac{\tau^x}{\rho} \right)_t - \frac{1}{c^2} \left(\frac{\tau y}{\rho} \right)_{tt} . \quad (14)$$

Solutions of this equation can be represented in terms of dispersive and nondispersive baroclinic Rossby waves (McCreary, 1976). A further wave like solution of Eqs. (7a) through (7c) is the equatorially trapped Kelvin wave (Moore and Philander, 1977). This solution can be wave like solution of Eqs. (7a) through (7c) is the equatorially trapped Kelvin wave (Moore and Philander, 1977). This solution can be derived more easily by constraining the meridional velocity to be zero

in the homogeneous ($\bar{\tau}=0$) part of (7a) and (7b) (also with $A=0$). The resulting Kelvin wave solution is a non-dispersive, eastward propagating wave with phase speed, c (Moore and Philander, 1977). Since this latter wave has zero north-south transport, it cannot alter the meridional heat transport pattern. However, it might be indirectly important through excitation of meridionally propagating, coastally-trapped Kelvin waves. Equatorial Kelvin waves have been shown to propagate part of their energy in the form of boundary trapped Kelvin waves (Moore, 1968).

III. Results and discussion

a. Net meridional transport

In the preceding section we discussed a relation that enables to estimate meridional heat fluxes from the interface depth of our model. To interpret the results an analysis of the heat budget components is in order. For a zonally integrated ocean, if one defines:

Q_s = storage of heat in the ocean (rate of gain or loss of heat),

Q_w = horizontal advection of heat by the wind driven circulation,

Q_t = horizontal advection of heat by the thermohaline circulation,

Q_{sfc} = net input or loss of heat through the ocean surface,
the heat budget for a particular body of water can be stated symbolically by the equation:

$$Q_s = Q_w + Q_t + Q_{sfc} \quad (15)$$

For a long-term average, since the ocean maintains a constant temperature, the storage term, Q_s in (15), can safely be neglected. At low latitudes, as noted before, the ocean receives a net input of heat through its surface, and hence, in order to balance this net input the advection terms, $Q_w + Q_t$, can be expected to be poleward.

The net heat transport estimated from the model via (8) is thought to represent the adiabatic advection of heat by the wind driven circulation (Q_w). Only Q_w is estimated in this study. The model does not include the transport due to the thermodynamic circulation or the surface heat fluxes. Unless, otherwise indicated, a reference to the net heat transport in the following sections is a reference to Q_w not to the "total" horizontal transport ($Q_w + Q_t$).

The 18-year average heat transport, computed using (8a), is shown in Fig. 2 as a function of latitude. North of 6°N the net transport is northward, while south of this latitude the transport is to the south. The cross-equatorial heat transport is from the northern to the southern hemisphere with a magnitude of about 0.18 PW.

Three regions can be identified in Fig. 2:

- i) From the southern boundary of the model (12°S) to around 5°N , the heat transport increases linearly from -0.35 PW at 12°S to -0.15 PW at around 5°N .
- ii) A turning latitude band from 5°N to about 8°N , where the transport changes from southward to northward.
- iii) To the north of 8°N the transport remains more or less constant at about 0.25PW until 12°N where it decreases slowly to the north.

Except for the "abnormal" latitudinal band north of the equator, our estimates imply a "normal" ocean in the sense introduced by Stommel (1980): one in which the flux of heat is poleward. Wyrтки

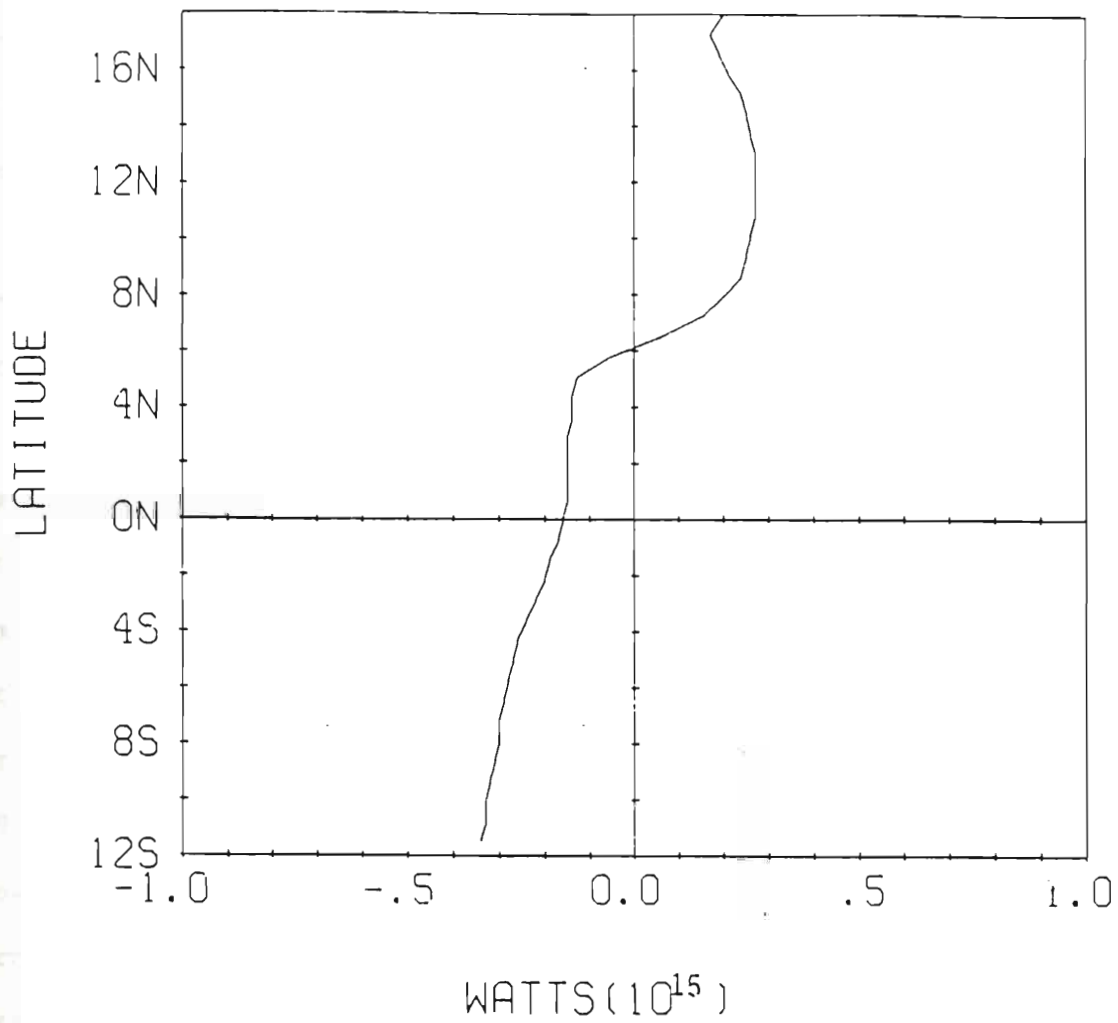


Fig. 2 Mean net meridional heat transport by the ocean model.
 Northward transport positive. Units in PW (1 PW = 10¹⁵W).

(1965) states that for heat balance calculations, the boundary between the north and south Pacific ocean should not be at the geographic equator but at the thermal equator which is situated near 6°N . If the thermal equator, instead of the geographic equator, is considered in Stommel's definition of a normal ocean, our "abnormal" band would be removed and our estimates would imply a completely normal Pacific Ocean.

Our estimates compare well with those calculated indirectly by Hastenrath (1980) from heat budget and radiation considerations. In both cases, there is a southward cross-equatorial heat transport of similar strength ($\sim 0.20\text{PW}$) and a turning latitude at about the same latitude; "somewhat north of the equator" (Hastenrath, 1980), 6°N in our case. Estimates with a numerical model presented by Meehl et al. (1982) forced by monthly mean winds and atmospheric temperatures also show very similar values for the cross-equatorial transport and turning latitude. The magnitudes of the transport at higher latitudes, however, are somewhat smaller in our study. Bryan (1982a) used the January-July average as an index of the seasonal variability in the heat transport. In Fig. 3 our January-July average is compared to Bryan's results. The similarity of both calculations is striking if one considers the very different characteristics of the models. The model used by Bryan (1982a) is a fully non-linear model with thermodynamic effects included and much greater vertical resolution than the one used in this study. The conclusion drawn from this thermodynamic effects included and much greater vertical resolution than the one used in this study. The conclusion drawn from this

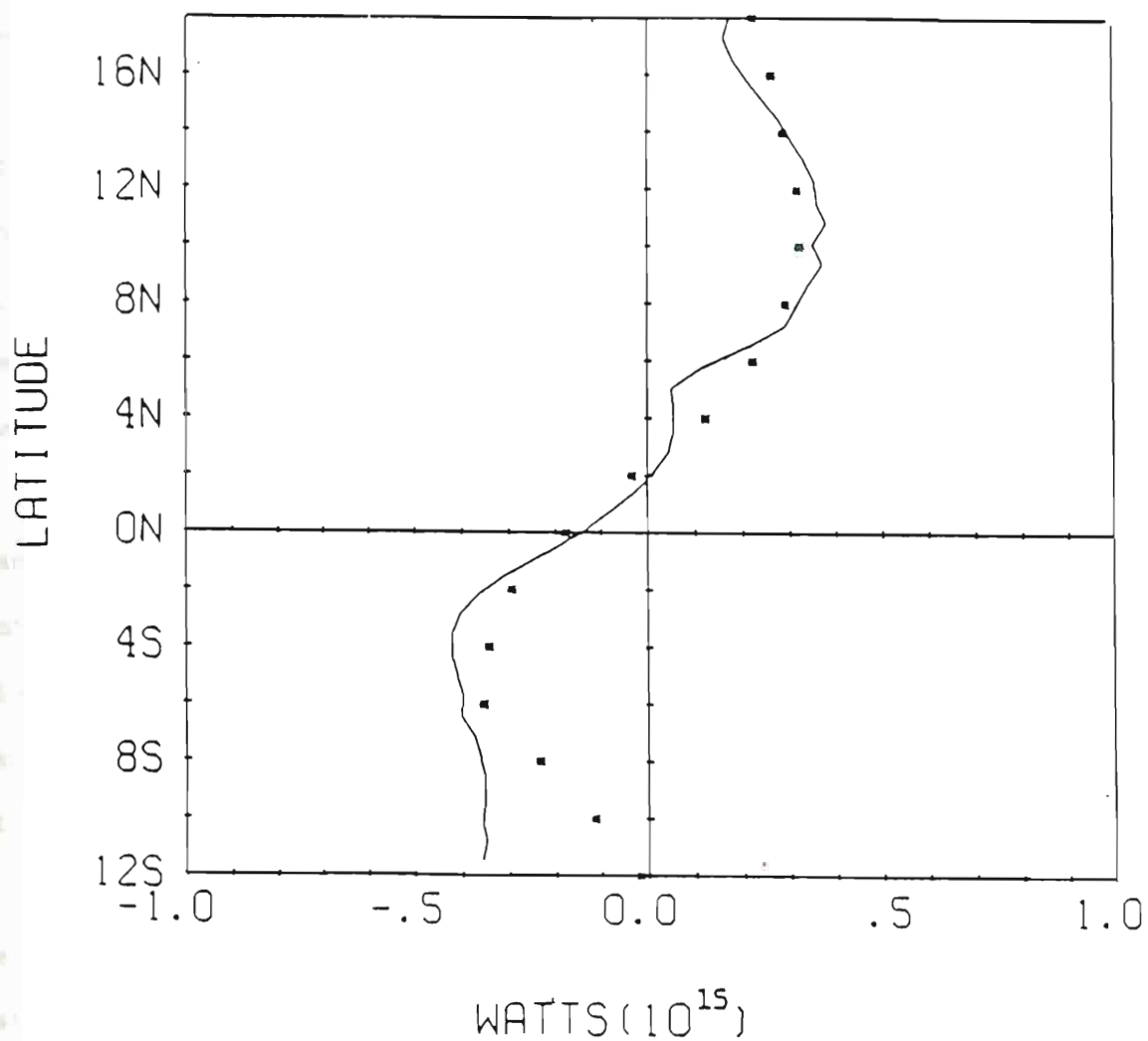


Fig. 3 January-July average heat transport by the ocean model (full line) compared to the January-July estimates from Bryan (1982a) (dots). Units are in PW.

result is that the heat storage and lateral heat advection play a dominant role in the overall heat budget in the equatorial Pacific over the seasonal time scale. In terms of the heat budget components in (15), comparison of our estimated heat transport with other estimates from global heat budget or models that includes thermodynamics imply a comparison of Q_w from our model to estimates of $Q_w + Q_t$, the fact that both quantities are similar, probably indicate that the wind driven advection in the tropical Pacific dominates over the advection by the thermodynamic circulation.

For the equatorial Pacific, earlier estimates of the net heat transport, based on heat-balance studies, tend to show little similarities, even in the direction of the transport (Emig, 1967). This is because at low latitudes the divergence of OHT is estimated as a small difference of very large quantities. Hastenrath (1980) estimates that a systematic error of 10 Wm^{-2} in the oceanic divergence of heat transport (a possible one) could lead to an error of the order of 1 PW in the transport around 30°N . As noted by Hastenrath, this figure cautions against too much optimism on the values of heat transport estimated from presently available satellite derived data, especially in the tropics. Unfortunately, no direct estimate of zonally averaged heat transport has been made for the equatorial Pacific to compare meaningfully with our results. Most of the literature on models which estimated the values of heat transport, present the results for the entire ocean regime on the earth (e.g. the literature on models which estimated the values of heat transport, present the results for the entire ocean regime on the earth (e.g.

Bryan et al., 1975; Manabe et al., 1979; Bryan, 1979; Bryan and Lewis, 1979), and cannot be directly compared with our estimates.

Fig. 4 shows the Ekman and geostrophic contributions to the net heat transport (4a and 4b respectively). Not surprisingly, since the average winds are easterlies (Fig. 5), the average Ekman transport is poleward at all latitudes (Fig. 4a). The geostrophic transport is equatorward at all latitudes (Fig. 4b). It should be noted that the order of magnitude for both contributions is 10 PW, one order of magnitude bigger than the net transport. Ekman and geostrophic transports nearly cancel each other with their "small" difference in magnitude giving rise to their combined contribution to the net transport shown in Fig. 4c. If one compares Fig. 4c with the net transport (replotted in Fig. 4d for comparison), one observes that, except near the equator, the net transport is almost exclusively due to the combined effect of the Ekman and geostrophic parts, as suggested by (10).

The three regions mentioned before for the net transport are more evident in the combined Ekman and geostrophic parts (Fig. 4c). It appears from Figs. 4a-4d that the change from positive to negative transport at the "turning band" around 6°N , is mainly due to an increase in the equatorward geostrophic transport while the Ekman transport remains more or less constant.

From south of 6°N to the equator, the geostrophic transport dominates, resulting in a net equatorward transport, while north of

From south of 6°N to the equator, the geostrophic transport dominates, resulting in a net equatorward transport, while north of 6°N and in the southern hemisphere, Ekman dominates, giving its

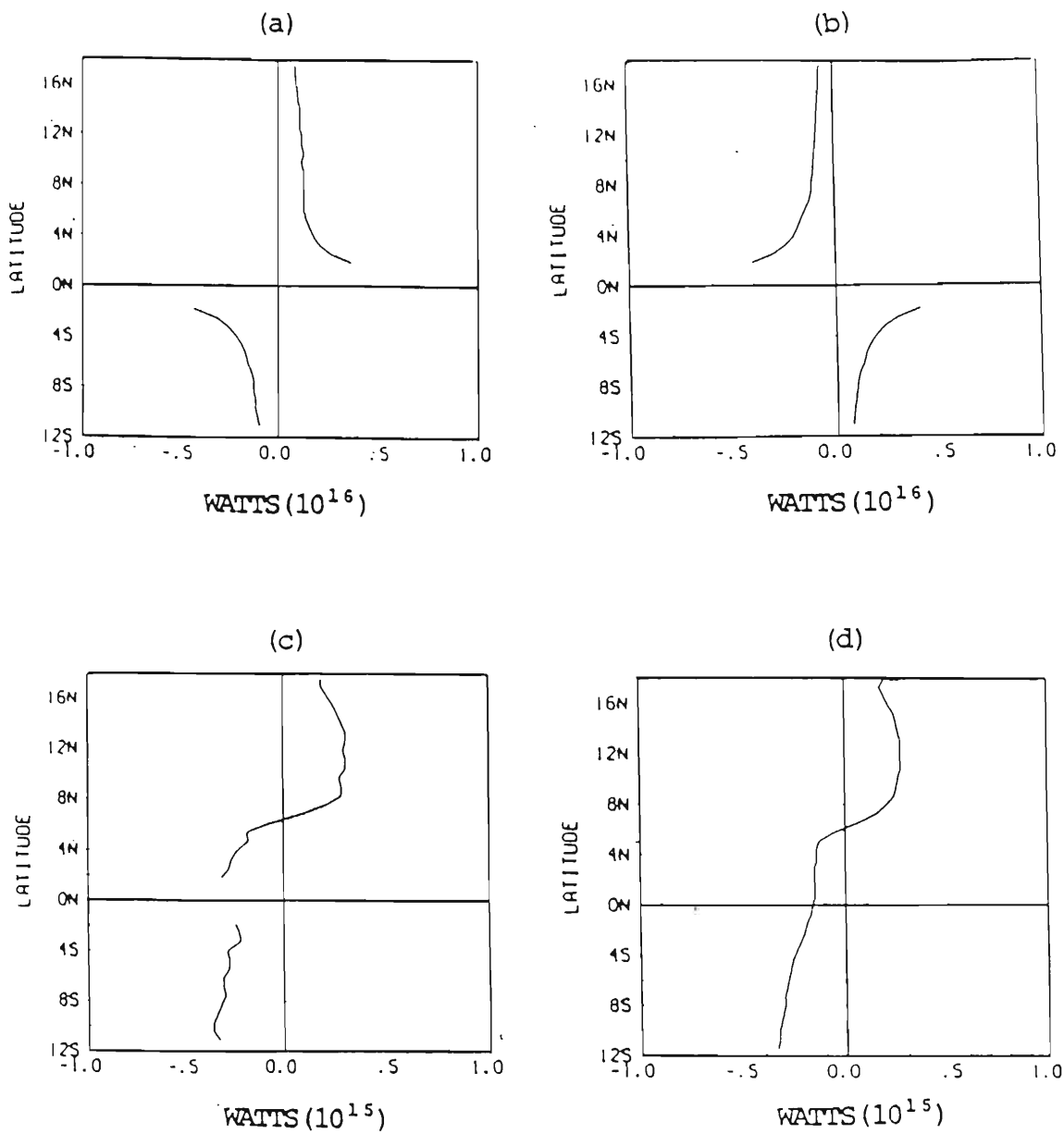


Fig. 4 Mean meridional heat transport due to: (a) Ekman effect (b) geostrophic effect; (c) Ekman + geostrophic; (d) net transport. See text for definitions. Note different units for a-b and c-d.

for a-b and c-d.

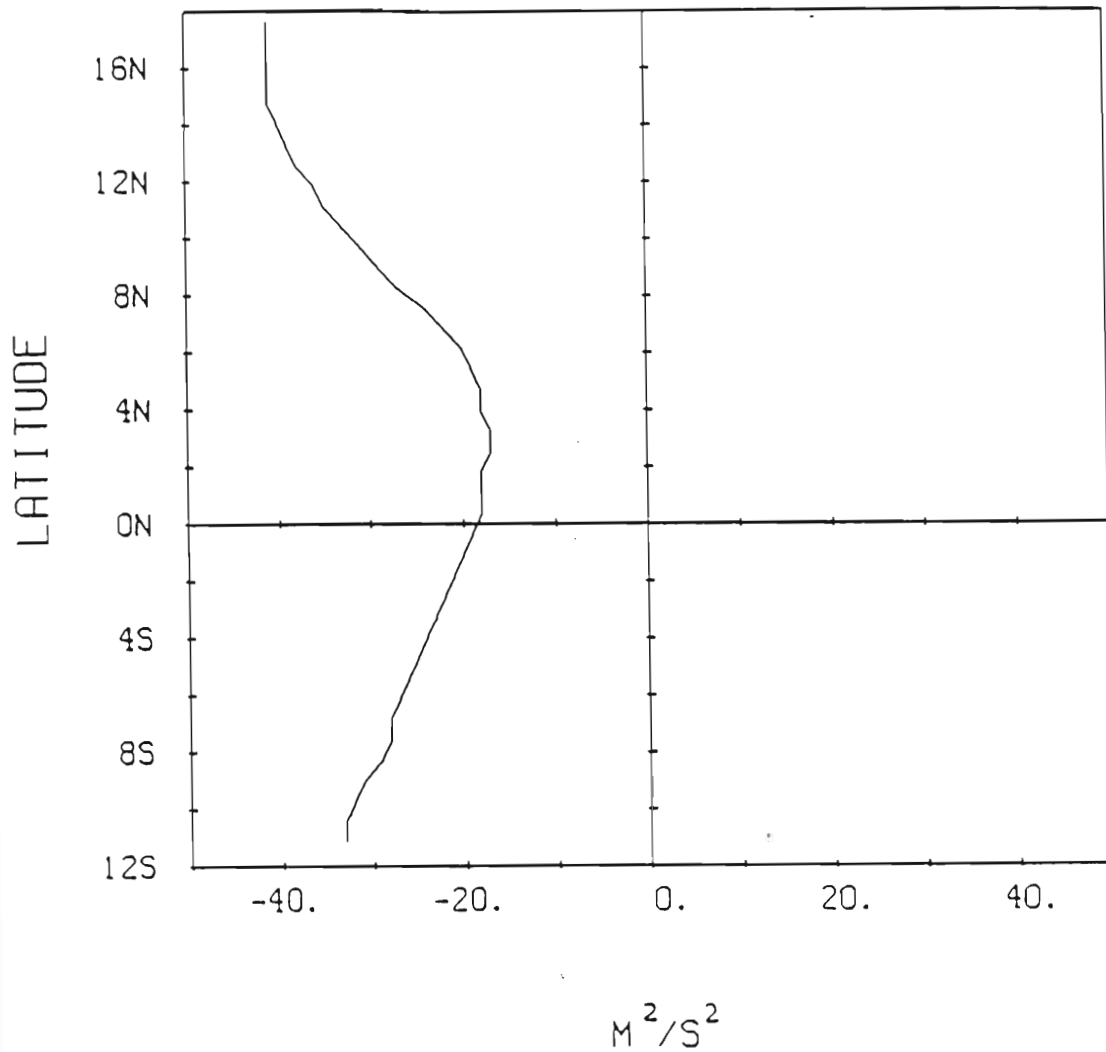


Fig. 5 Zonally averaged mean east-west pseudo wind stress (wind magnitude times wind component (Goldenberg and O'Brien, 1981)). Negative values indicate westward winds. Units are in m^2s^{-2} .

poleward (normal-sign) characteristic to the heat transport in the tropical Pacific.

The general agreement between our estimates and those computed from heat balance and radiation considerations (e.g. Emig, 1967; Hastenrath, 1980) seem to confirm the dominant role played by the adiabatic advection in the tropical Pacific Oceanic heat transport. Adiabatic advection is the only heat transporting mechanism included in our model.

The thermohaline circulation that would result from the meridional distribution of surface fluxes and that could also contribute to the meridional heat transport, is probably too weak to make an important contribution to this area of the Pacific. For the Atlantic, the thermohaline circulation is thought to be the dominant mechanism (Hastenrath, 1980; Stommel, 1980; Bryan, 1982b). The characteristics of the heat transport for the Pacific and Atlantic oceans are, consequently, very different. While the Pacific, as mentioned before, transports heat away from the equator (normal-sign ocean), the transport in the Atlantic is northward at all latitudes (abnormal-sign in the southern hemisphere) (Hastenrath, 1980). The difference has been explained in terms of the thermohaline circulation in the Atlantic (Stommel, 1980). The Atlantic loses sufficient heat in the North Atlantic that it causes the heat flux from the South Atlantic to be reversed in sign (Stommel, 1980). Since the Pacific Atlantic to be reversed in sign (Stommel, 1980). Since the Pacific

does not extend to such high latitudes in the northern hemisphere, the thermohaline circulation is weaker, and does not constitute a dominant mechanism for transporting heat. It is possible, however, that a reason for our values being smaller than those computed by Hastenrath (1980) and Meehl et al. (1982), is the absence of the thermohaline circulation in our model. The effect of the thermohaline circulation in the Pacific trade wind regions, would be to reinforce the Ekman drift, producing a stronger poleward transport of surface water (Bryan et al., 1975), hence, a stronger poleward transport of heat.

Transport of heat in a horizontal plane (i.e. gyral effect) and the contribution to the ocean heat transport by synoptic scale eddies have been shown to be negligible in the equatorial regions (Bryan and Lewis, 1979).

b. Seasonal variation

Oort and Vonder Haar (1976) showed evidence of a large seasonal variation of the OHT. They found the amplitude of the annual variation in the tropical ocean to be of the order of 10 PW. Since the mean heat transport at low latitudes is of the order of 1 PW, it can be easily concluded that this huge seasonal oscillation dominates the characteristics of the transport in the tropical ocean and, hence, plays an important role in the overall heat budget calculations and climate.

Merle (1980) studied the seasonal heat budget in the equatorial climate.

Merle (1980), studying the seasonal heat budget in the equatorial Atlantic, found that the seasonal variation in the rate of heat

storage is about an order of magnitude greater than (and out of phase with) the seasonal variation of the net input of heat through the air-sea interface. The interpretation given by Merle (1980) is that, the redistribution of heat is associated with the dynamical response of the ocean to seasonal changes in surface winds rather than through a local surface heating balance. There have not been similar studies for the equatorial Pacific, but the estimated values of heat transport and storage by most investigators (e.g. Oort and Vonder Haar, 1976; Shopf, 1980; Bryan, 1982b) point to the same conclusion.

Using a numerical model of the world ocean (Bryan, 1979; Bryan and Lewis, 1979) Bryan (1982a) described the seasonal variation of the meridional heat transport in the Atlantic and Pacific Oceans. With the January minus July pattern as representative range of the annual cycle, he found the vertical overturning associated with the Ekman transport to be the dominant term in the overall equatorial meridional transport. Bryan (1982a) estimated the northward equatorial transport to vary from about +1 PW in January to about -1 PW in July.

The effect of long planetary waves on the seasonal heat transport was studied by Shopf (1980). Using a simple numerical model, Shopf (1980) demonstrated that, although these waves strongly affect the local behavior, they do not significantly modify the zonally integrated transport. The equatorial and extra-equatorial dynamics in our model (Eqs.(7a) through (7c)), as noted before, include long planetary waves. Specifically, close to the equator, our model (Eqs.(7a) through (7c)), as noted before, include long planetary waves. Specifically, close to the equator, our model

response includes dispersive and nondispersive Rossby waves as well as the equatorially-trapped Kelvin wave. The results of Shopf (1980) suggest that, at the seasonal time scale at least, and for the zonally integrated transport all these waves are not relevant and the solution across the equator is simply determined by continuity requirements.

Following is a brief description of the characteristics of the wind used to force the model to provide background for the discussion on the seasonal variation of the estimated heat transport. A more extensive description of the wind in the area was given by Wyrcki and Meyers (1975) and by Goldenberg and O'Brien (1981).

Seasonal variation of the zonally averaged east-west wind pseudo stress is shown in Fig. 6a as a function of latitude and month. Fig. 6b shows a similar plot for the wind stress anomaly, calculated by subtracting from the values in Fig. 6a the annual average wind at each latitude.

As seen in Fig. 6a, the zonal component of the wind is towards the west throughout the year at all latitudes. An annual oscillation is present with maximum easterlies ($-58\text{m}^2\text{s}^{-2}$) at 10°N and at 12°S ($-42\text{m}^2\text{s}^{-2}$) in February and August, respectively, and weaker easterlies in September at around 8°N ($-3\text{m}^2\text{s}^{-2}$). From Fig. 6b, the zonal component of the wind shows a seasonal variation markedly antisymmetric across the equator with stronger than the average antisymmetric across the equator with stronger than the average

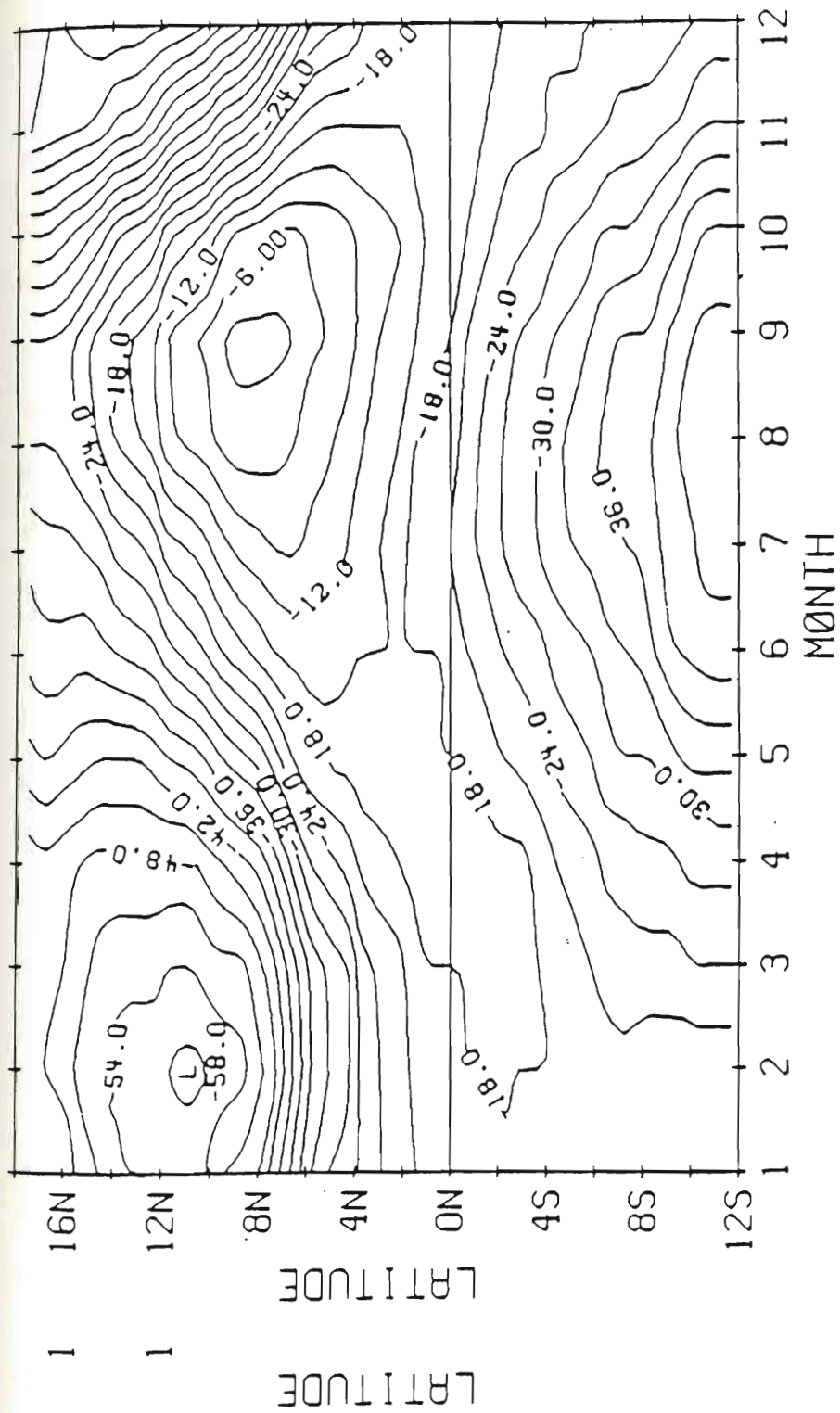


Fig. 6a Monthly mean zonally average east-west wind pseudo stress.
 Positive values indicates eastward winds. Units are in m^2s^{-2} .
 Contour interval is $3 \text{ m}^2\text{s}^{-2}$.

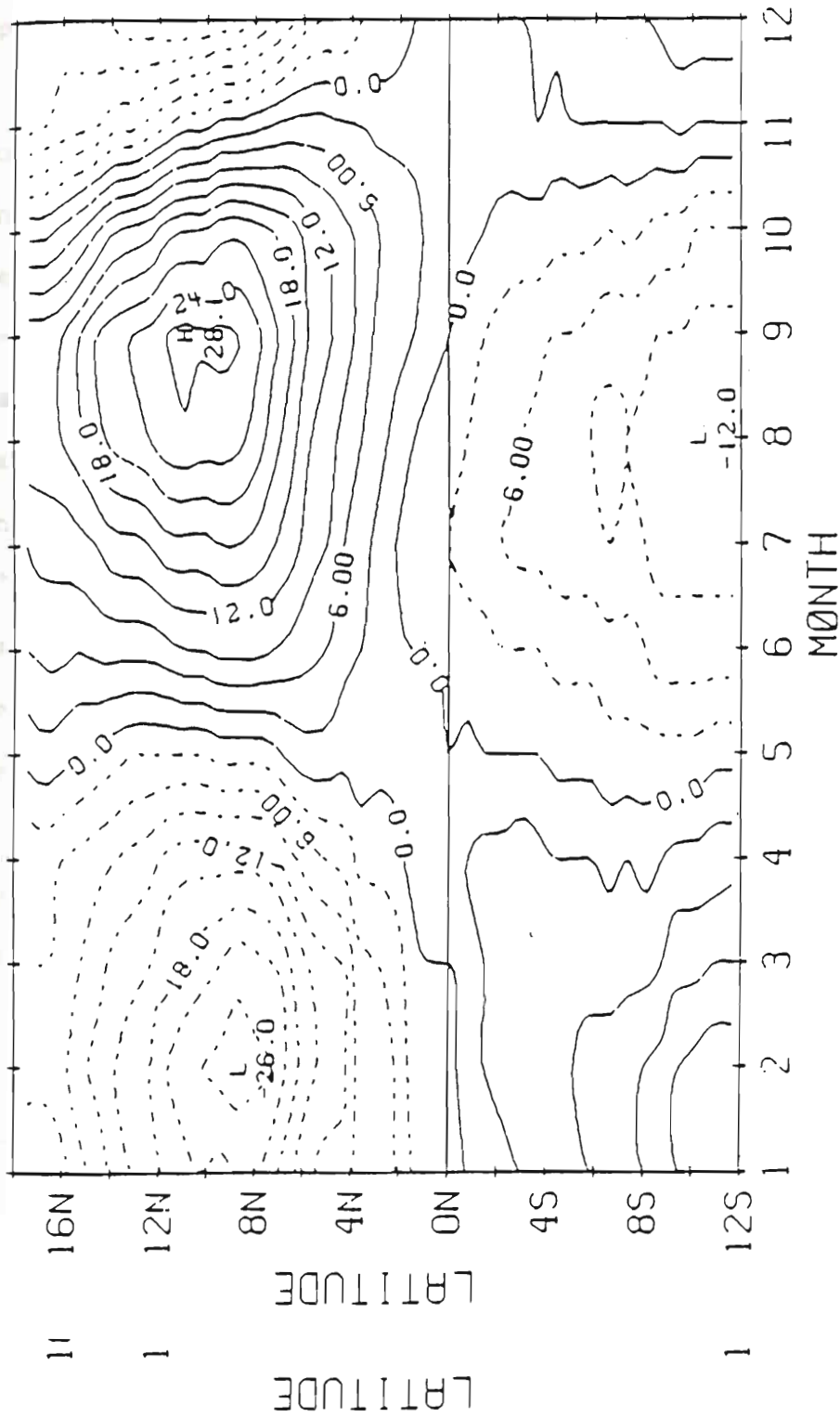


Fig. 66 Monthly mean zonally averaged east-west wind stress anomaly. Zonal mean at each latitude has been removed. Negative contours (dash lines) indicate stronger than average easterlies. Contour interval is $3 \text{ m}^2 \text{ s}^{-2}$.

easterlies in the winter-spring hemisphere and weaker than the average in the summer-fall hemisphere. The magnitude of the annual variation appears strongest around 8-10°N and weakest at the equator.

Fig. 7 shows the seasonal variation of heat transport as a function of latitude and time. There is a strong seasonal variation in the OHT, with a maximum northward heat transport (NHT) at 8°N in February and a maximum southward heat transport (SHT) in September at around 5°N. The band from 5°N to 8°N is the band of maximum annual variation going from 1.4 PW in February to -1.1 PW in September. The magnitude of the heat transport decreases to the north and south of these latitudes, becoming less positive (northward) away from around 8°N in the northern hemisphere winter-spring and less negative (southward) in the northern hemisphere fall-summer. In the southern hemisphere the transport is mostly to the south with a relative maximum SHT in July.

The cross-equatorial transport is from the summer to the winter hemisphere. From December to April there is a northward cross-equatorial heat transport, while from May to November a southward cross-equatorial heat transport is present.

The Ekman and geostrophic components of the heat transport are shown in Figs. 8 and 9, respectively. As expected, they oppose each other, with Ekman transport poleward and geostrophic transport equatorward in both hemispheres throughout the year.

equatorward in both hemispheres throughout the year.

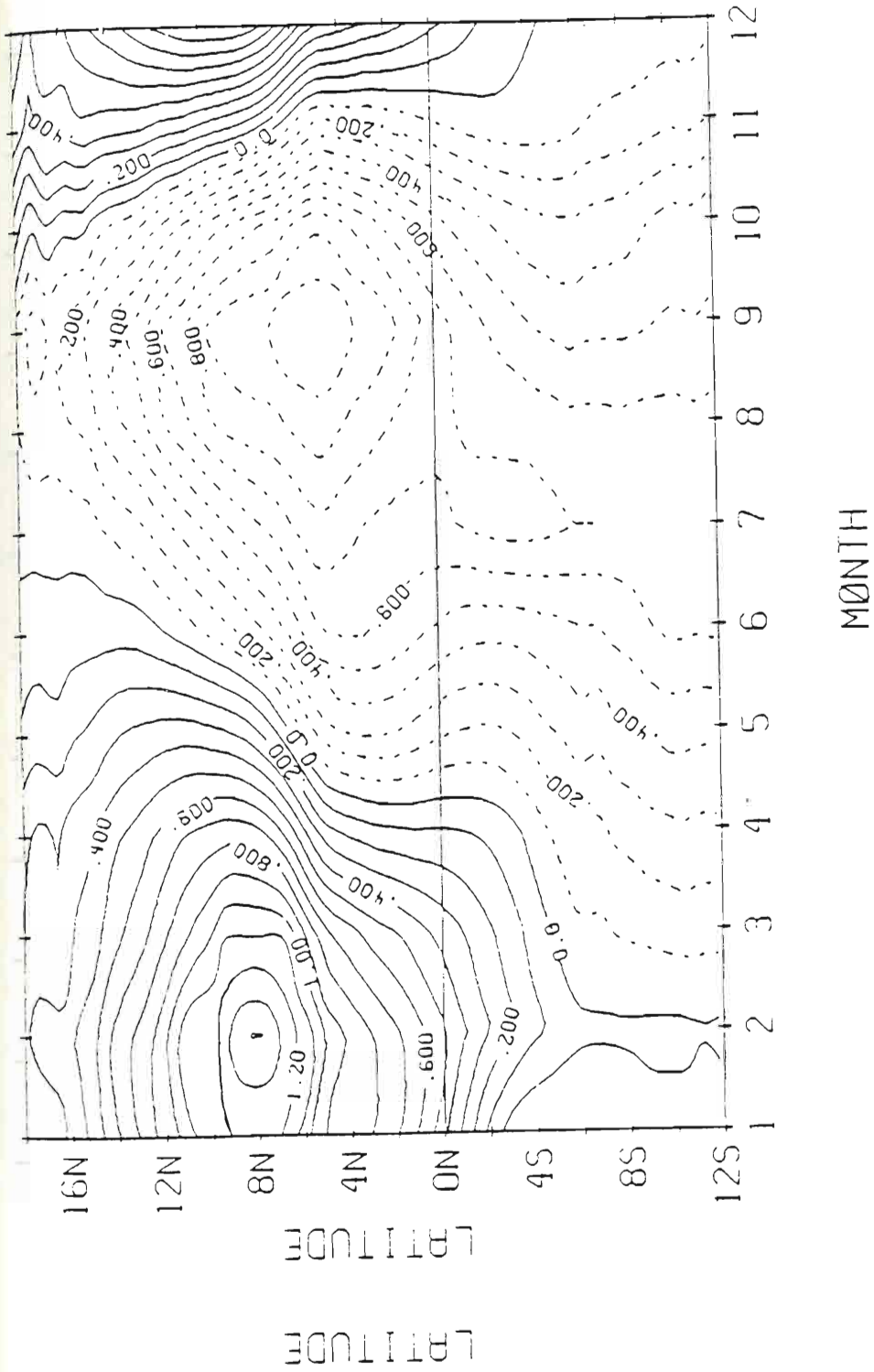


Fig. 7 Annual cycle of net meridional heat transport. Positive contours indicate northward transport. Units are in PW. Contour interval is .1 PW.

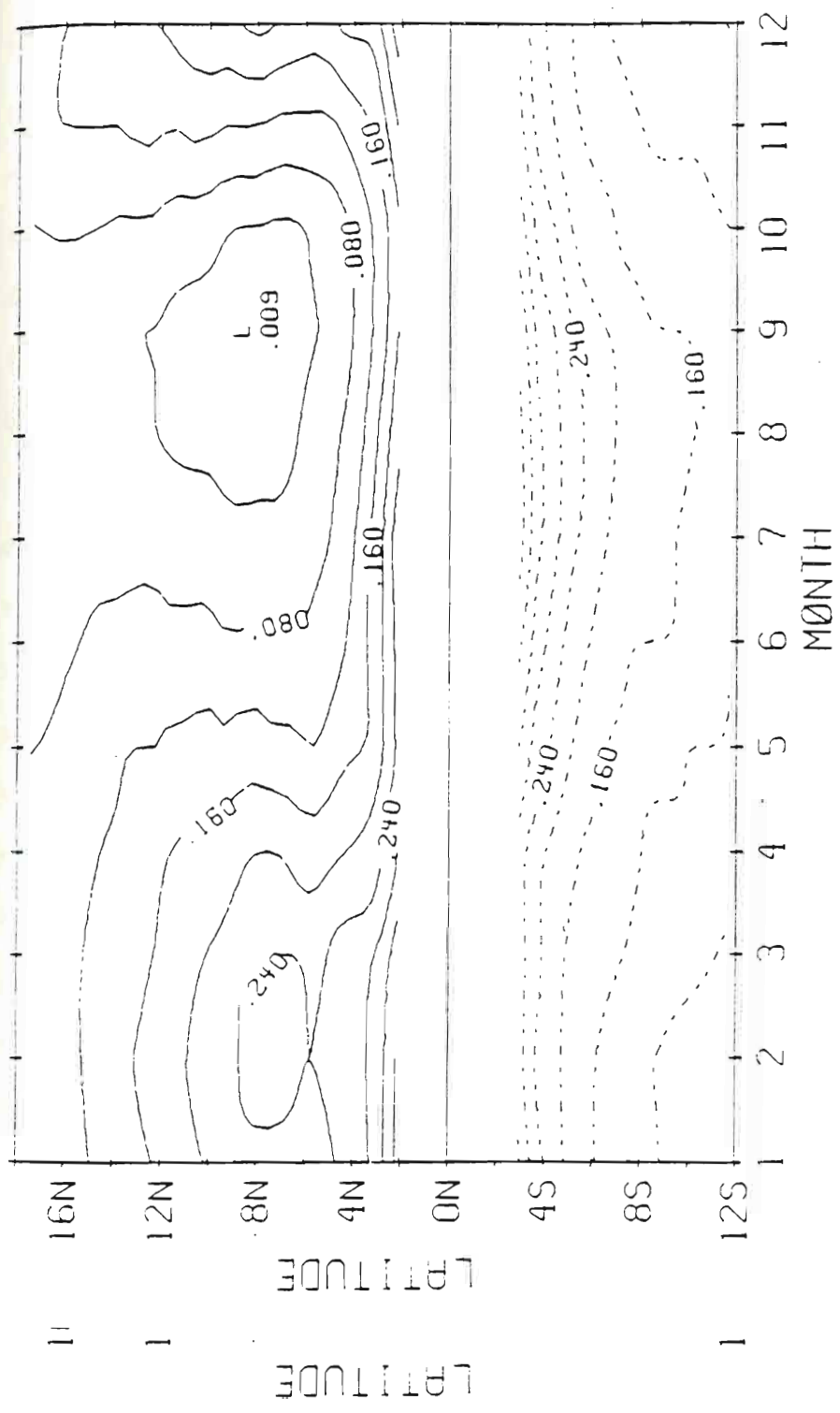


Fig. 8 Annual cycle of meridional heat transport due to Ekman transport. Positive contours indicate northward transport. Units are in PW time $10^{16}W$. Contour interval is .4 PW.

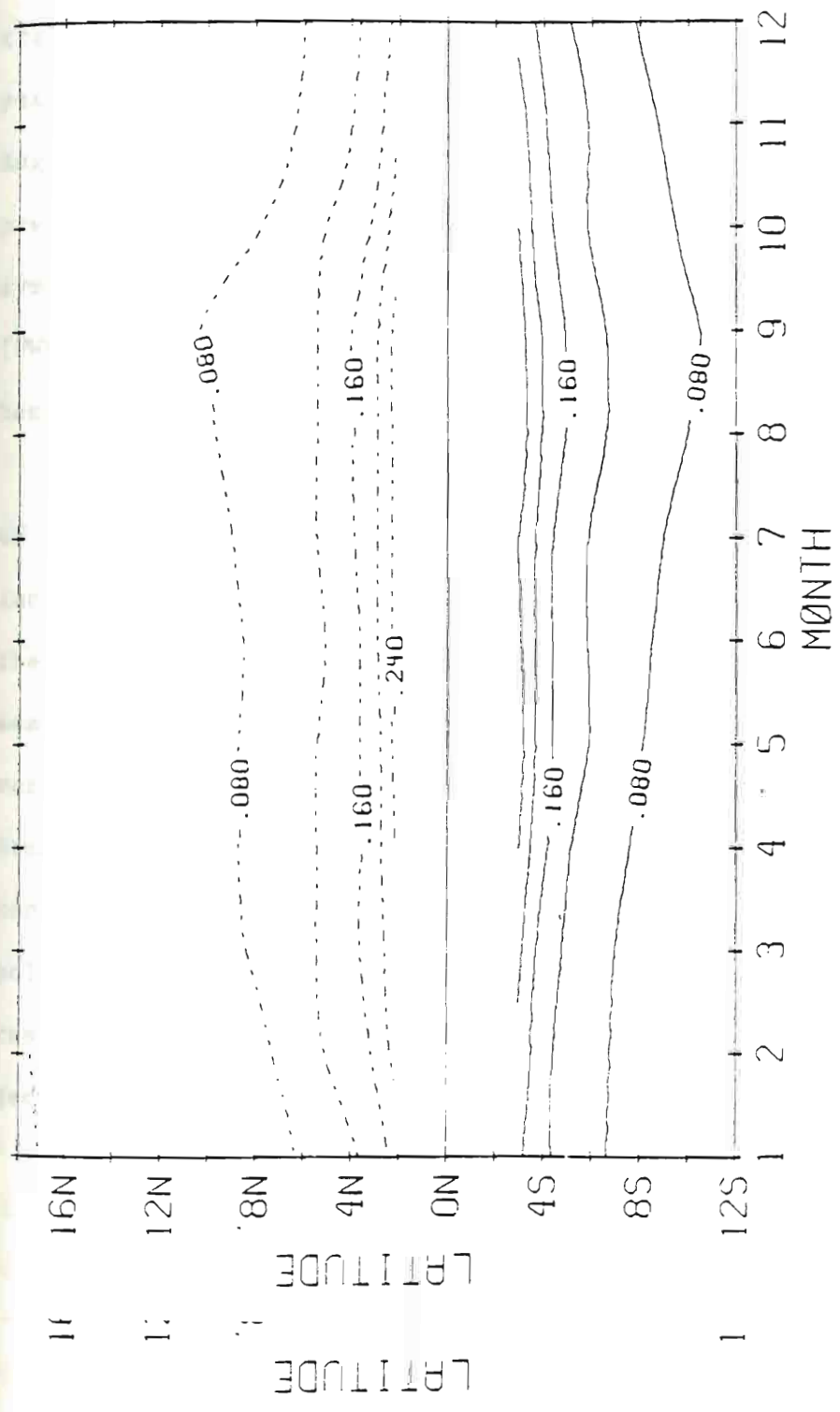


Fig. 9 Annual cycle of meridional heat transport due to geostrophic transport. Positive contours indicate northward transport. Units are in 10^{16} Watts.

The geostrophic transport (Fig. 9) is nearly antisymmetric across the equator, it increases in magnitude toward the equator in a way dictated by the reduction of the Coriolis parameter (Eq. (13)). The transport, at a given latitude, remains almost constant throughout the year except for a slight increase on the equatorward transport in August-September. The Ekman transport (Fig. 8), on the other hand, presents a marked seasonal variation. The transport is more or less symmetric across the equator with weak poleward heat transport (PWHT) in August-September and strong PWHT in February in the northern hemisphere and vice versa for the southern hemisphere.

The importance of the Ekman transport on the seasonal variation of net heat transport becomes evident by comparing Figs. 6 and 8. It can be seen from those figures that, away from the equator, almost all the seasonal variation in the net transport is given by a similar seasonal variation in the Ekman transport associated with the seasonal variation in zonal wind. The stronger easterlies in the winter hemisphere (Fig. 5b) drive a stronger poleward Ekman transport that can overcome the equatorward geostrophic transport resulting in a net poleward transport. In the summer hemisphere, the reduced easterlies result in a weaker poleward Ekman transport and the equatorward geostrophic transport dominates.

c. Interannual variation

In the preceding section it was shown that the seasonal variation of the winds in the tropical Pacific is responsible for the seasonal variation of the meridional heat transport and that its effect is very strong compared to the mean transport. In the tropical Pacific the interannual variations in the wind stress can be as strong as the seasonal variations. For example, in their study of the wind stress variability, Goldenberg and O'Brien (1981) found an area of high interannual variability centered just north of the equator in the central Pacific. It seems only reasonable to expect the meridional heat transport to respond to such large-scale interannual variations in the wind pattern as well as to the seasonal variations. In this section, a description of the interannual variability of the estimated heat transport is made.

During recent years the recognition of the El Nino phenomenon as a part of the very large scale anomalies in both the atmosphere and the ocean has produced a dramatic increase in the interest on the phenomenon as can be judged by the large amount of literature published on the subject. In this study, it is not our intention to analyze in detail the El Nino events in our estimates of heat transport but only to describe the interannual variability of the estimated heat transport and to recognize that it must be a part of the large-scale variability in the ocean-atmosphere system associated with El Nino events.

Historically, the term El Nino refers to an annual occurrence of warm water off the coast of Peru and Ecuador. At irregular intervals a massive version of El Nino occurs, where the warm water accumulation is excessive, leading to a natural catastrophe. This irregular and more dramatic event is what recently has been referred to as the El Nino phenomenon. The interannual variability of the model response (including El Nino events) in the 60's and 70's have been discussed by Busalacchi and O'Brien (1981) and Busalacchi et al. (1983). The model response was found to correlate very well with the observed sea level records.

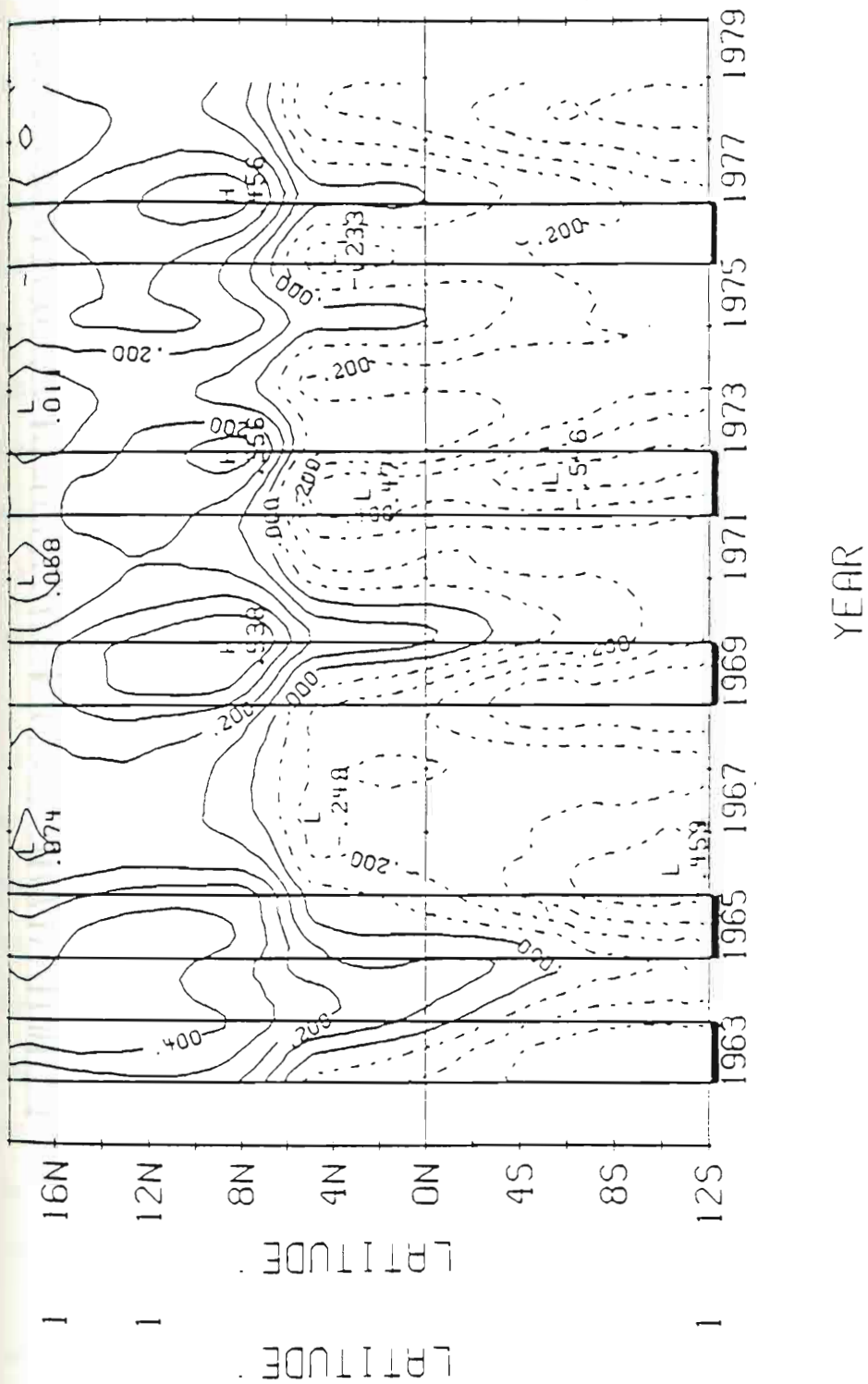
Probably because of historical reasons, what have been referred to as El Nino characteristics are mostly related to eastern boundary responses (i.e., warming of the sea surface, higher sea level, deepening of the thermocline, etc.). The response of the model (and presumably of the real ocean), however, is characterized by longitudinal variation (Busalacchi et al., 1983). A zonally integrated meridional heat transport is the response of the whole basin, and it is difficult to recognize the dynamical mechanisms that have been usually linked to the El Nino phenomenon (i.e. equatorial and coastally trapped Kelvin waves).

Intuitively, one would expect a decrease in the poleward heat transport during the onset and development of El Nino event, when the ocean at the eastern boundary is warming and the pycnocline is deepening. During the retreat of the warm water, the final stages of ocean at the eastern boundary is warming and the pycnocline is deepening. During the retreat of the warm water, the final stages of

the phenomenon, an increase in the poleward transport can be expected in order to bring the pycnocline depth and heat transport back to its "normal" averaged position.

The interannual variability of the estimated heat transport is obtained by applying a 12-month running mean filter to the computed time series. The result is shown in Fig. 10a as a latitude-time plot. Fig. 10b shows the heat transport anomalies as a function of latitude and time. A positive anomaly means stronger northward transport or weaker southward transport than the long-term average. A negative anomaly means a weaker northward transport or a stronger southward transport compared to the long-term mean. In Figs. 10a and 10b, the years that have been classified as El Nino years (1963, 1965, 1969, 1972, 1976) are marked to facilitate the description.

Inspection of Figs. 10a and 10b shows an important result of this section: the interannual variability in the estimated meridional transport is not at all negligible and is not restricted to the equator. The actual amplitude of the variability is bigger at some latitudes than the mean and almost as large as the seasonal variation. This result itself implies that estimated values of heat transport based on the direct method (e.g. Hall and Bryden, 1982) do not necessarily represent the "true" long term average. Long-time series are called for to define a meaningful average annual transport.



F Fig. 10a Interannual variability of the net meridional heat transport obtained by filtering with a 12-month running mean. The years that have been classified as El Niño years are shaded in the figure. Units are in PW. Contour interval is .1 PW.

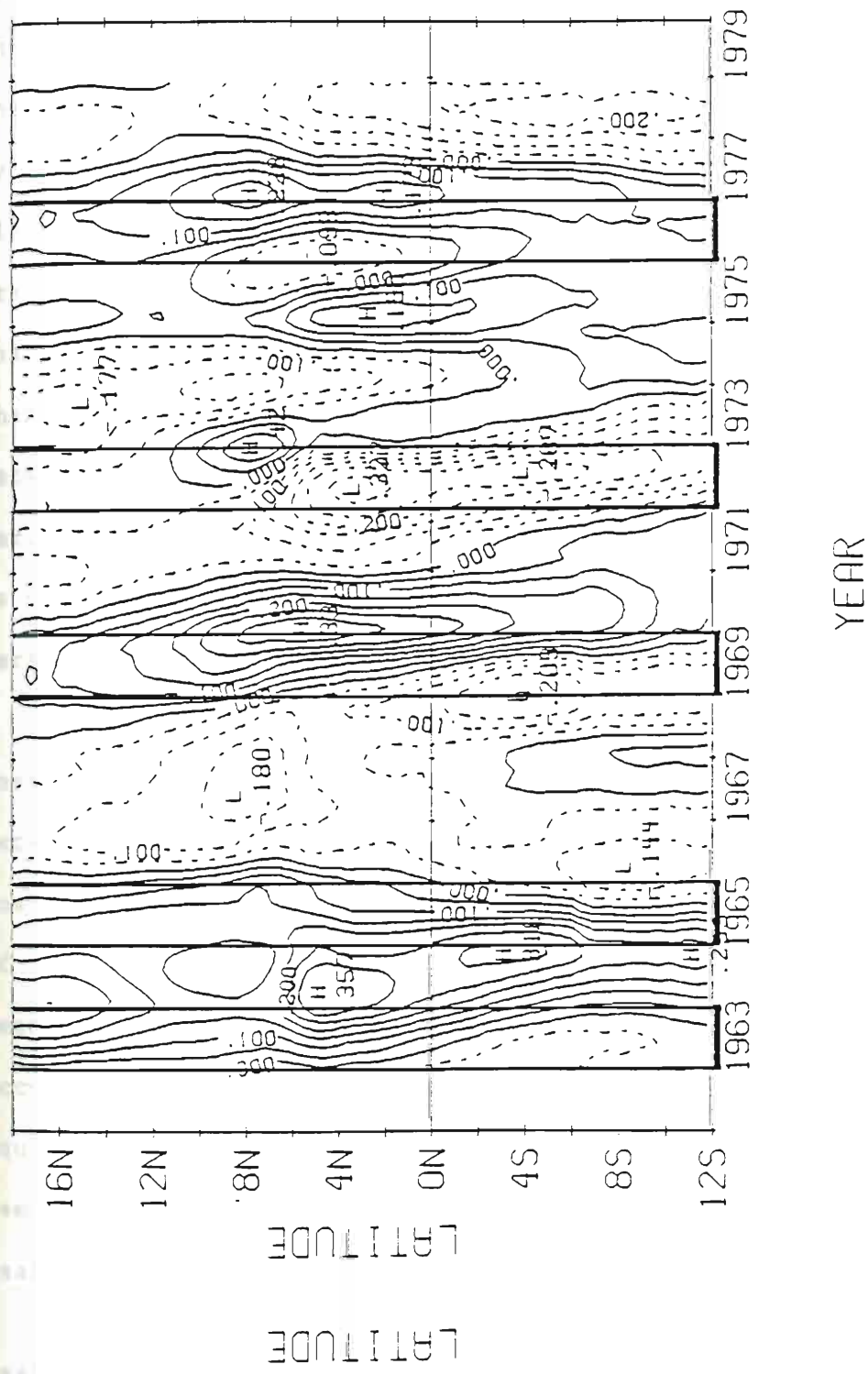


Fig. 10b Same as Fig. 10a, but for the heat transport anomaly.

From Fig. 10a the region of maximum interannual variability is found to be around 8°N . This latitude corresponds approximately to the latitude of maximum seasonal variability, which seems to reinforce the idea of the interannual variability being linked to the seasonal cycle. To corroborate this idea, complex demodulation (see Bloomfield, 1976) of the heat transport time series at the annual frequency were performed (not shown here). The complex demodulation analysis showed that the interannual variation is mainly due to changes in the amplitude of the annual cycle which explains the link between the two time scales. Interpretation of interannual variability in terms of an anomalous amplification of the annual cycle is not new. It has been discussed by Horel (1982) for atmospheric parameters and by Meyers (1982) for oceanic parameters.

From Fig. 10b it can be seen that the anomalies are not restricted to the equator. Bands of positive and negative anomalies extend throughout the whole latitudinal extent of the model. Maximum positive anomalies north of the equator occur at the end (beginning of next year) of 1963, 1969, 1972, 1976, all of these years having been classified as El Nino years. Another positive anomaly maxima occur north of the equator at the beginning of 1975 and south of the equator at the end of 1964 (beginning of 1965). The year 1975 has been classified as an aborted El Nino year and 1965 as a major El Nino year (Rasmusson and Carpenter, 1982).

year (Rasmusson and Carpenter, 1982).

Although the latitudinal locus, strength and duration of the maximum positive anomalies differ for each event. Fig. 10b shows a clear correlation between the occurrences of El Nino and the heat transport anomalies. For 1963, 1965, 1969 the pattern seems to be a stronger-than-average poleward heat transport; positive anomalies in the north and negative anomalies in the south. The strongest latitudinal variation on the heat transport anomalies occurs at around 5°N in 1972, a year that has been recognized as a major El Nino (Rasmusson and Carpenter, 1982). For this year a region of convergence anomaly, negative anomaly to the north of a positive anomaly, also occurs to the north of 8°N .

IV. Summary and Conclusions

Net meridional heat transport in the equatorial Pacific has been estimated with a simple numerical model. The model used is that of Busalacchi and O'Brien (1980, 1981): A linear, reduced-gravity model in an equatorial β -plane forced by 18 years of monthly surface winds (from January 1962 to December 1979). The coastline geometry of the model basin is an approximation of the tropical Pacific. With a linear equation of state, the density difference between the dynamically active upper layer and the motionless lower layer was related to a difference in temperature and heat content.

The estimated long-term mean heat transport by the wind-driven circulation was first analyzed. Our estimated heat transport was found to be southward to the south of 6°N and northward north of this latitude. Qualitatively, the latitudinal shape and magnitude of the transport compares well with the results presented by Hastenrath (1980) and Meehl et al. (1982) which shows that the lateral advection is a major term in the total heat budget. However, the different characteristics of previous models to the model used in this study (e.g. realistic geometry, real winds) and the lack of dense enough observations (in space and time) make it impossible to carry out a detailed comparison of our results with previous studies of heat observations (in space and time) make it impossible to carry out a detailed comparison of our results with previous studies of heat transport.

The physical mechanisms involved in heat transport were investigated by decomposing the net meridional heat transport into two parts: Ekman and geostrophic. These two components oppose each other, with poleward and equatorward transport for the Ekman and geostrophic components, respectively. Both, Ekman and geostrophic components, were found to be an order of magnitude larger than their sum. Except near the equator the net heat transport is almost exclusively due to the combined effect of the Ekman and geostrophic parts. The mechanism suggested by these results is that of an equatorward geostrophic transport of water maintained by a west-to-east pressure gradient which is balanced by the easterly trade winds, opposed by a direct poleward Ekman drift. The resulting net meridional transport of water in the upper (warmer) layer is compensated by an equal transport of lower layer (colder) water producing a net meridional heat flux.

Seasonal and interannual variations are found to be large compared to the long-term mean. At the seasonal time scale the geostrophic transport remains more or less constant and large seasonal variations in the estimated heat transport were found to be directly associated with the seasonal variation of the zonal wind via Ekman transport. The stronger-than-average easterlies in the winter hemisphere drive a stronger poleward Ekman transport than can overcome the equatorward geostrophic transport, resulting in a net poleward heat transport. In the summer hemisphere, the reduced easterlies the equatorward geostrophic transport, resulting in a net poleward heat transport. In the summer hemisphere, the reduced easterlies

result in a weaker poleward Ekman transport and the equatorward geostrophic transport dominates.

Maximum interannual variability was found to be north of the equator, at a latitude that approximately coincides with the latitude of maximum seasonal variability. Interpretation of the interannual variability as an anomalous intensification of the annual cycle is thought to explain this coincidence. Correlation between the occurrence of El Nino phenomenon and the interannual anomalies in the estimated heat transport is evident. The most conspicuous being the presence of large positive anomalies at the end of all the years classified as El Nino years. It is interesting to note that the interannual variations associated with El Nino events are not restricted to the near-equatorial region.

It is recognized that the model used in this study is a very simple one. The present model only provides information on heat storage and lateral heat advection, two important but not exclusive terms on the total heat budget. A complete, thermodynamic model could only shed information on the remaining terms of the heat budget. Inclusion of surface heat fluxes and other thermodynamics would certainly modify the magnitude and probably the phase of our estimated heat transport. However, comparison between our results and previous estimates based on observations and numerical models which incorporate

thermodynamics, suggests that the adiabatic dynamics, with near cancellation of the Ekman and geostrophic transports is a dominant process in the total heat budget of the equatorial Pacific. Of course, it would be of interest to test this idea with a more complete model.

REFERENCES

- Bryan, K., 1979: Models of the world ocean. Dyn. Atmos. Oceans., 3, 327-338.
- _____, 1982a: Seasonal variation in meridional overturning and poleward heat transport in the Atlantic and Pacific Ocean: a model study. J. Mar. Res., 40, (supplement) 39-53.
- _____, 1982b: Poleward heat transport by the ocean: Observations and models. Ann. Rev. Earth Planet. Sci., 10, 15-38.
- _____, 1983: Poleward heat transport by the ocean. Rev. Geophys. Space Phys., 21, 1131-1137.
- _____, and L. D. Lewis, 1979: A water mass model of the world ocean. J. Geophys. Res., 84, 2503-2517.
- _____, S. Manabe and R. C. Pacanowski, 1975: A global ocean-atmosphere climate model. Part II. The oceanic circulation. J. Phys. Oceanogr., 5, 30-46.
- Budyko, M. I., 1963: Atlas of the Heat Balance of the Earth. Moscow, Globnaia Geofiz. Observ., 69pp.
- Busalacchi, A. J., and J. J. O'Brien, 1980: The seasonal variability in a model of the Tropical Pacific. J. Phys. Oceanogr., 10, 1929-1951.
- _____, and J. J. O'Brien, 1981: Interannual variability of the Equatorial Pacific in the 1960's. J. Geophys. Res., 86, 10901-10907.
- _____, K. Takeuchi and J. J. O'Brien, 1983: Interannual variability of the Equatorial Pacific - Revisited. J. Geophys. Res., 88, 7551-7562.
- Cane, M. A., and E. S. Sarachik, 1981: The response of a linear baroclinic equatorial ocean to periodic forcing. J. Marine Res., 39, 651-693.
- _____, and E. S. Sarachik, 1983: Seasonal heat transport in a baroclinic equatorial ocean to periodic forcing. J. Marine Res., 39, 651-693.
- _____, and E. S. Sarachik, 1983: Seasonal heat transport in a forced equatorial baroclinic model. J. Phys. Oceanogr., 13, 1744-1746.

- Emig, M., 1967: Heat transport by ocean currents. J. Geophys. Res., 72, 2519-2529.
- Goldenberg, S. B., and J. J. O'Brien, 1981: Time and space variability of Tropical Pacific wind stress. Mon. Wea. Rev., 109, 1190-1207.
- Hall, M. M., and H. L. Bryden, 1982: Direct estimates and mechanisms of ocean heat transport. Deep Sea Res., 29, 339-359.
- Hastenrath, S., 1980: Heat budget of tropical ocean and atmosphere. J. Phys. Oceanogr., 10, 159-170.
- _____, and P. Lamb, 1977: Climatic Atlas of the Tropical Atlantic and Eastern Pacific. Madison: University of Wisconsin Press, 105pp.
- Horel, J. D., 1982: On the annual cycle of the tropical Pacific atmosphere and ocean. Mon. Wea. Rev., 110, 1863-1878.
- Manabe, S., K. Bryan, and M. J. Spelman, 1979: A global ocean-atmosphere climate model with seasonal variation for future studies of climate sensitivity. Dyn. Atmos. Oceans, 3, 393-426.
- McCreary, J., 1976: Eastern tropical response to changing wind systems: with application to El Nino. J. Phys. Oceanogr., 6, 632-645.
- Meehl, G. A., W. M. Washington, and A. J. Semtner, 1982: Experiments with a global ocean model driven by observed atmospheric forcing. J. Phys. Oceanogr., 12, 301-312.
- Merle, J., 1980: Seasonal heat budget in the Equatorial Atlantic Ocean. J. Phys. Oceanogr., 10, 464-469.
- Meyers, G., 1982: Interannual variation in sea level near Truk Island--A bimodal seasonal cycle. J. Phys. Oceanogr., 12, 1161-1168.
- Moore, D. W., 1968: Planetary-gravity waves in an equatorial ocean. Ph.D. Thesis, Harvard University, Cambridge, Massachusetts, 207 pp.
- _____, and S. G. H. Philander, 1977: Modeling of the tropical oceanic circulation, in The Sea, Vol. 6, 319-361. Interscience, New York.
- _____, oceanic circulation, in The Sea, Vol. 6, 319-361. Interscience, New York.

- Oort, A. H., and T. Vonder Haar, 1976: On the observed annual cycle in the ocean-atmosphere heat balance over the northern hemisphere. J. Phys. Oceanogr., 6, 781-800.
- Schopf, P. S., 1980: The role of Ekman flow and planetary waves in the oceanic cross-equatorial heat transport. J. Phys. Oceanogr., 10, 330-341.
- Stommel, H., 1980: Asymmetry of interoceanic fresh-water and heat fluxes. Geophysics, 77, 2377-2381.
- Vonder Haar, T., and A. H. Oort, 1973: New estimates of annual poleward energy transport by northern hemisphere oceans. J. Phys. Oceanogr., 2, 169-172.
- Wyrтки, K., 1965: The average annual heat balance of the North Pacific Ocean and its relation to ocean circulation. J. Geophys. Res., 70, 4547-4559.
- _____, and G. Meyers, 1975: The trade wind field over the Pacific Ocean. Part I. The mean field and the mean annual variation. Rep. HIG-75-1, Hawaii Inst. Geophys., Univ. of Hawaii, Honolulu.

APPENDIX

List of Symbols

A	Horizontal eddy viscosity coefficient, $10^2 \text{ m}^2 \text{ s}^{-1}$.
B	Northward net heat transport.
B_E, B_g	Ekman and geostrophic component of heat transport, respectively.
c	Baroclinic phase speed, $(g'H)^{1/2}$, 2.45 ms^{-1} .
c_p	Heat capacity of water at constant pressure, $4.02 \times 10^3 \text{ J kg}^{-1}$.
g	Acceleration due to gravity, 9.8 ms^{-2} .
g'	Reduced gravity, $g(\rho_0 - \rho)/\rho_0$,
h	Upper layer thickness.
H	Initial upper layer thickness, 300m.
\hat{k}	z-directed unit vector.
s, S	Heat content.
t	Time.
T, T_0	Temperature of upper and lower layer, respectively.
x, y, z	Tangent plane cartesian coordinates: x positive eastward, y positive northward and z positive upward.
x_0, x_{00}	Meridional boundaries of the model basin. eastward, y positive northward and z positive upward.
x_0, x_{00}	Meridional boundaries of the model basin.

- α Coefficient of thermal expansion, $2.4 \times 10^{-4} \text{ deg}^{-1}$.
- β Meridional derivative of Coriolis parameter,
 $2.25 \times 10^{-11} \text{ m}^{-1} \text{ s}^{-1}$.
- γ Constant coefficient $\Delta\rho c_p \alpha^{-1}$.
- ρ, ρ_0 Density of sea water, upper and lower layer,
respectively.
- $\Delta\rho$ Density difference between upper and lower layer,
 2.0 kg m^{-3} .
- τ^x, τ^y Zonal and meridional components of wind stress,
respectively.